Gas-Phase Reactions of Homo- and Heteronuclear Clusters MM'^+ (M, M′ = Fe, Co, Ni) with Linear Alkanenitriles

by **Maria Schlangen**, **Detlef Schröder**, and **Helmut Schwarz***

Institut für Chemie, Technische Universität Berlin, Straße des 17. Juni 135, D-10623 Berlin
(fax: (+49)30-314-21102; e-mail: Helmut.Schwarz@mail.chem.tu-berlin.de)

Dedicated to *Rolf Huisgen* in admiration of his inspiring work on physical organic chemistry

Fourier-transform ion-cyclotron-resonance mass spectrometry is used to investigate the reactions of mass-selected homo- and heteronuclear clusters MM'^+ (M, M′ = Fe, Co, Ni) with linear alkanenitriles. The reactions with pentanenitrile are examined in detail by means of deuterium-labeling studies. In comparison to the previously studied atomic cations Fe^+, Co^+, and Ni^+, the diatomic cluster cations react more specifically and only insert in C–H bonds in the initial step, whereas the bare ions M^+ activate both C–H and C–C bonds. Like for the atomic cations, dehydrogenation proceeds *via remote functionalization* of the terminal positions of the substrate, although H-scrambling processes, preceding dehydrogenation, are more pronounced for the dinuclear cluster cations. The Ni-containing cluster cations $CoNi^+$ and Ni_2^+ are unique in that they bring about double dehydrogenation as well as activation of C–C bonds subsequently to the first dehydrogenation. The latter kind of reaction is also partly observed for the $[RCN - H_2]$-complexes of $FeCo^+$, Co_2^+, and $FeNi^+$ in their secondary reactions with pentanenitrile. The behavior of the Fe-containing cluster cations Fe_2^+ and $FeCo^+$ is more subtle compared to that of the Ni-containing clusters Ni_2^+ and $CoNi^+$ as well as that of homonuclear Co_2^+. Based on extensive labeling experiments, dehydrogenation of pentanenitrile by these cluster cations follows a 1,2-elimination mode, whereas loss of H_2 from the Fe_2^+ and $FeCo^+$ complexes of the substrate proceeds to some extent *via* a 1,1-elimination involving the unactivated Me group of the substrate. A more quantitative description of the labeling distribution has been achieved by extensive modeling.

Introduction. – Exploitation of the distinct chemical character of transition metals, owing to their unique electronic configuration, constitutes the basis of heterogeneous catalysis. Although the *d*-block elements offer a wide variety of catalytic properties, this versatility is confronted with an enormous number of chemical problems, which often prevent the realization of a catalytic sequence. Variation of surface textures and the combination of different transition metals are, among others, possible means to enhance the performance and to enlarge the number of given catalytic systems. For example, synergistic effects of different transition metals proved to bring about efficient C–N coupling reactions in gas-phase experiments with bimetallic cluster cations not being achieved by their homonuclear analogues [1]. Because surface defects often constitute the active sites for chemical reactions, support-free transition-metal clusters may serve as a model to study the intrinsic properties of catalysts. As demonstrated earlier, gas-phase studies provide a powerful experimental approach to assess the inherent reactivities of the cluster ions under well-defined conditions without being obscured by difficult-to-control solvation, aggregation, counterions, and other effects [2]. Finally, combinations of different transition metals are used not only in homogeneous and heterogeneous catalysis [3], but often also in, *e.g.*, metallo-proteins to accomplish specific chemical reactions for a given substrate [4].

Activation of C–H and C–C bonds constitutes in many cases the crucial step in catalytic cycles and has also been observed in the reactions of bare transition-metal ions with organic substrates in the gas phase. More than a decade ago, we were able to demonstrate that the selective functionalization of C–H and C–C bonds spatially separated from the site of complexation can be achieved in gas-phase organometallic chemistry [5]. These features are also characteristic for enzymatic processes, and *Breslow* has coined the term *remote functionalization* for a reaction in which precoordination precedes selective bond activation far away from the complexed group [6]. In this particular respect, one of the best-studied gas-phase systems are alkanenitriles (RCN) [5]. According to extensive quantum-chemical calculations, the initial complexation of a coordinatively unsaturated transition-metal ion M^+ occurs in an *end-on* fashion to the CN group; this step is followed by an internal solvation of the ion with the consequence that certain segments of the otherwise conformationally flexible backbone are exposed to interact intramolecularly with M^+ [5][7]. In connection with extensive gas-phase studies on *remote functionalization*, the reactions of atomic Fe^+, Co^+, and Ni^+ with pentanenitrile occupy a special position in that they reveal a highly metal-specific chemistry [5b,c] (see next *Sect.*). Analogous processes of the corresponding homo- and heteronuclear cluster ions MM'^+ with pentanenitrile (and shorter nitriles) have not been investigated so far, and obvious questions are among others: *i*) Do the reactions of the homonuclear cluster cations M_2^+ exhibit patterns similar to those of the atomic cations M^+ (M = Fe, Co, Ni), and which sort of gas-phase chemistry is expected for the heteronuclear cluster cations MM'^+ (M, M′ = Fe, Co, Ni)? *ii*) Do heteronuclear dimers MM'^+ in their reactivities conform to the one observed for the atomic systems M^+ and M'^+ or do they show a fundamentally different chemistry, as reported previously in a different context [1] and anticipated in a more generalized manner in an earlier account [5a]?

Reactions of Fe^+, Co^+, and Ni^+ with Pentanenitrile. To put the current study in a proper context, a schematic representation of the dehydrogenation and the elimination of ethene by atomic Fe^+, Co^+, and Ni^+ from pentanenitrile in line with the *remote functionalization* concept is given in *Scheme 1* [5b,c]. Starting from the internally 'solvated' coordination complex **1**, dehydrogenation can take place either by initial insertion in a primary or, alternatively, in a secondary C–H bond; the first option leads eventually to the endocyclic multi-center transition state (MCTS) **6**, while the second one results in the exocyclic MCTS **5**. In the course of ethene elimination, it is obvious that, at one stage of the multi-step process, C–C bond activation has to occur, either in the initial step (**1** → **4**) or in the course of a β-alkyl migration after C–H bond insertion (**3** → **7**), followed by the formation of endocyclic (**7**) or exocyclic (**8**) transition structures as the energetically most-demanding species. Based on extensive computational studies of nonanenitrile/Fe^+ and nonanenitrile/Co^+ [7a,b], endocyclic MCTSs were found to be disfavored in general, *i.e.*, for both dehydrogenation as well as the elimination of ethene, and the reaction channels passing through exocyclic structures prevail for longer alkanenitriles [7a,b]. For the shorter pentanenitrile, the situation is, perhaps not entirely unexpectedly, more complex, and despite extensive experimental studies an *a priori* judgement about the preferred pathways (*i.e.*, **1** → **2** → **5** → **9** *vs.* **1** → **3** → **6** → **9**, and **1** → **3** → **7** → **10** *vs.* **1** → **4** → **8** → **10**, resp.) cannot be given. While for pentanenitrile/M^+, the activation of C–H/C–C bonds closer to the CN group

(structures **2** and **4** in comparison to **3**) – resulting in more favorable exocyclic transition structures – can be considered as an advantage, this path may be inhibited due to an energetically demanding distortion of the linear arrangement R–CN–M^+. Actually, while the exocyclic transition structures of nonanenitrile/Fe^+ and nonanenitrile/Co^+ are generally more favored by *ca.* 40 kJ mol^{-1} in comparison to endocyclic transition structures, the distortion from the 180° *end-on* conformation in M–N–C requires *ca.* 30 kJ to 60 kJ mol^{-1} depending on the degree of bending [7a]. Obviously, for smaller systems there may well exist a balanced situation due to the operation of opposing effects.

Scheme 1. *Mechanisms of Dehydrogenation* (**1** → **2** → **5** → **9**, and **1** → **3** → **6** → **9**, resp.) *and for the Elimination of Ethene* (**1** → **3** → **7** → **10**, and **1** → **4** → **8** → **10**, resp.) *According to the Concept of* Remote Functionalization

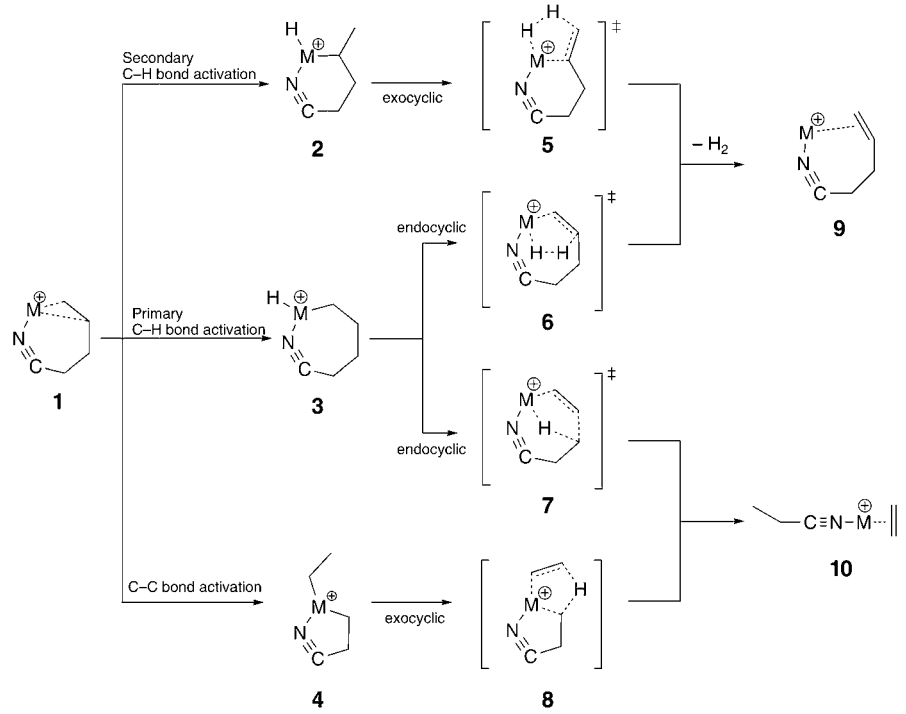

In terms of overall product formation, the reactions of Fe^+, Co^+, and Ni^+ with pentanenitrile are similar, although the branching ratios differ (*Table 1*). For Fe^+ and Co^+, dehydrogenation represents the main product channel, whereas elimination of propene is clearly preferred for Ni^+.

As to the detailed mechanisms of C–H/C–C-bond activation on *n*-C_4H_9CN, the results obtained with the isotopomers **11a**–**11d** (*Fig. 1*) were quite revealing in that they are not compatible whith the simplified, traditional mechanism depicted in *Scheme 1* [5b,c]. Surprisingly, the labeling studies indicated that the expulsion of ethene originates only for Ni^+ – and not for Fe^+ and Co^+ – exclusively from the γ and δ positions of the alkyl chain as required for the concept of *remote functionalization*. In

Table 1. *Reactions of the Atomic Metal Cations Fe^+, Co^+, and Ni^+ with Pentanenitrile*[a])[b])

		Fe	Co	Ni	
$M^+ + n\text{-}C_4H_9CN$	$[MC_5H_9N]^+$		7	11	(1)
	$[MC_5H_7N]^+ + H_2$	76	58	22	(2)
	$[MC_3H_5N]^+ + C_2H_4$	23	12	26	(3)
	$[MC_2H_3N]^+ + C_3H_6$	1	20	40	(4)
	$[MC_3H_6]^+ + C_2H_3N$		3	< 1	(5)

[a]) Data are taken from [5b]. [b]) Intensities of the products are normalized to 100%.

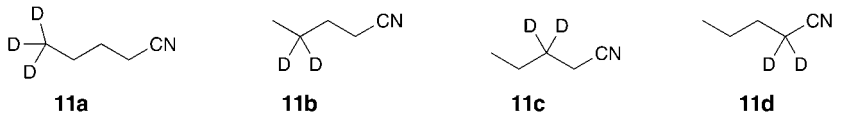

Fig. 1. *Isotopomers of pentanenitrile investigated*

contrast, ethene is eliminated from *internal* positions of the nitrile backbone (*Scheme 2*) in the case of Fe^+, and that holds true in part also for the loss of ethene from pentanenitrile/Co^+. In spite of this commonality, some subtle mechanistic differences exist between these two metal cations: while for Co^+ a direct ethene elimination path (**12** → **13** → **15**) is operative, partial equilibration of the α- and γ-CH_2 units of **12** is achieved, presumably *via* the intermediate **16**, in the case of Fe^+. Furthermore, while dehydrogenation proceeds *via remote functionalization* for all three metal ions, akin to the mechanism of ethene elimination, the losses of HD from **11d** (19%) and of H_2 from **11b** (29%) in the case of Fe^+ are again due to an equilibration of the α and γ positions of **12**, and the conceivable existence of a ferracyclobutane intermediate **16** accounts for the experimental findings.

Scheme 2. *Elimination of Ethene from* Internal *Positions of Pentanenitrile by Fe^+ and Co^+*. The ferracyclobutane intermediate **16** is suggested to bring about partial equilibration of the α and γ positions of $n\text{-}C_4H_9CN/Fe^+$.

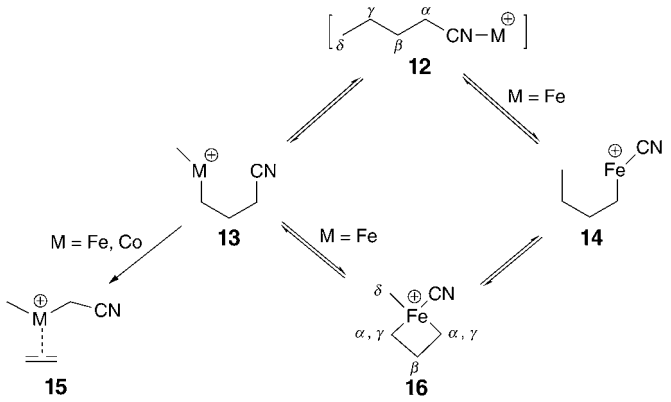

Experimental. – The present experiments were performed with a *Spectrospin CMS 47X FT-ICR* mass spectrometer [8] equipped with a *Smalley*-type [9] cluster ion source [10]. In brief, the beam of a pulsed Nd : YAG laser operating at 1064 nm is focused on a rotating pure metal or an alloy target to generate a hot metal plasma, from which cluster formation occurs by synchronization of a He pulse and subsequent supersonic expansion. After transfer of the thus produced ions by a set of potentials and ion lenses to the ICR cell, the cluster ions of interest are mass-selected by means of the FERETS ion-ejection protocol [11], thermalized by an Ar pulse, and then mass-selected again. The ion/molecule reactions of trapped cluster ions with the nitriles were then studied by leaking-in the neutral substrates at stationary pressures of the order of 10^{-8} mbar. Concerning the thermalization of the cluster cations, several observations reported in the present work and detailed investigations on Ni-cluster oxides [12] suggest that some electronically excited Ni_2^+ generated in the cluster source possibly survive the thermalization. This is supported by the observation of some reactions which are clearly endothermic for ground-state Ni_2^+ and should, therefore, not take place at ambient temperature.

The experimental second-order rate constants k are evaluated on the basis of the pseudo-first-order approximation with an absolute error of 30% [13]; in the determination of reaction-rate constants, the respective ion-gauge sensitivities [14] as well as calibration factors [13] were considered. Corresponding to capture theory [15], the reaction efficency ϕ is given by the ratio of the bimolecular rate constants k and the gas-phase kinetic collision rates k_c. In some consecutive reactions, the observed time dependencies of the product distributions are analyzed by means of kinetic modeling [16]. Furthermore, some reactions were studied by double-resonance experiments [17] that allow the identification of crucial intermediates in consecutive reaction sequences by continuous ejection of the assumed intermediate ion of interest from the ICR cell and its effect on the product distribution.

Results and Discussion. – *Dehydrogenation.* Whereas the bare metal cations Fe^+, Co^+, and Ni^+ activate both C–H and C–C bonds of pentanenitrile, the diatomic cluster cations MM'^+ react more specifically and insert exclusively in C–H bonds in the initial step (*Table 2*). Only after dehydrogenation, consecutive C–C bond activation is observed for $CoNi^+$ and Ni_2^+ as discussed further below. We note in passing that a preference for C–C bond activation has already been reported in different contexts for atomic cations of late transition metals in contrast to a predominant C–H bond activation by the corresponding diatomic cluster cations. For example, 65% of the products formed in the reaction of Ni^+ with butane are due to C–C bond activation, whereas Ni_2^+ dehydrogenates butane with a branching ratio of 80% [18]. Furthermore, the reactions of $FeCo^+$ with alkenes are restricted to C–H bond activation, whereas atomic Fe^+ and Co^+ activate C–H as well as C–C bonds of alkenes [19].

In line with the concept of *remote functionalization,* the labeling distribution of the dehydrogenation products reveal that, for all cluster cations examined, dehydrogenation involving the terminal positions (γ and δ) is preferred (*Table 3*). This result is supported by preliminary DFT studies performed on the cluster-cation complexes with ethanenitrile, according to which only the linear *end-on* C_{3v}-symmetric complexes, $CH_3CN–MM'^+$, correspond to minima [20]; linear *end-on* structures are also preferred for the mononuclear cations [7a,b]. However, some distinct features of the isotopic distribution in the reaction products are notable. For example, the unexpectedly high amount of H_2 loss from **11b** and the considerable fraction of D_2 elimination from **11a** for the nitrile complexes of Fe_2^+ and $FeCo^+$ cannot be reconciled in terms of *remote functionalization* by a formal 1,2-H_2 elimination. Thus, for these clusters an additional process needs to be invoked in the dehydrogenation, and a formal 1,1-elimination of H_2 involving the terminal C–H bonds is suggested to be operative (see below). Furthermore, H/D scrambling processes to different extents are observed for all the cluster cations examined. To quantitatively analyze these results, detailed kinetic

Table 2. *Reactions of the Homo- and Heteronuclear Cluster Cations MM'^{+}* (M, M′ = Fe, Co, Ni) *with Pentanenitrile*

$Fe_2^+ + n\text{-}C_4H_9CN$	$[Fe_2C_5H_9N]^+$	65%	(6)
	$[Fe_2C_5H_7N]^+ + H_2$	35%	(7)
$\Sigma\, k = 1.05 \cdot 10^{-9}$ cm^3 s^{-1}			
$\phi = 0.33$			
$Co_2^+ + n\text{-}C_4H_9CN$	$[Co_2C_5H_9N]^+$	74%	(8)
	$[Co_2C_5H_7N]^+ + H_2$	26%	(9)
$\Sigma\, k = 1.15 \cdot 10^{-9}$ cm^3 s^{-1}			
$\phi = 0.37$			
$Ni_2^+ + n\text{-}C_4H_9CN$	$[Ni_2C_5H_7N]^+ + H_2$	5%	(10)
	$[Ni_2C_5H_5N]^+ + 2\,H_2$	62%	(11)
	$[NiC_5H_9N]^+ + Ni$	5%	(12)
	$[Ni_2C_4H_6]^+ + [CH_3N]$	18%	(13)
	$[Ni_2C_3H_3N]^+ + [C_2H_6]$	10%	(14)
$\Sigma\, k = 2.13 \cdot 10^{-9}$ cm^3 s^{-1}			
$\phi = 0.68$			
$FeCo^+ + n\text{-}C_4H_9CN$	$[FeCoC_5H_9N]^+$	68%	(15)
	$[FeCoC_5H_7N]^+ + H_2$	32%	(16)
$\Sigma\, k = 1.1 \cdot 10^{-9}$ cm^3 s^{-1}			
$\phi = 0.35$			
$FeNi^+ + n\text{-}C_4H_9CN$	$[FeNiC_5H_9N]^+$	10%	(17)
	$[FeNiC_5H_7N]^+ + H_2$	80%	(18)
	$[NiC_5H_9N]^+ + Fe$	10%	(19)
$\Sigma\, k = 1.7 \cdot 10^{-9}$ cm^3 s^{-1}			
$\phi = 0.54$			
$CoNi_+ + n\text{-}C_4H_9CN$	$[CoNiC_5H_7N]^+ + H_2$	40%	(20)
	$[CoNiC_5H_5N]^+ + 2\,H_2$	25%	(21)
	$[NiC_5H_9N]^+ + Co$	25%	(22)
	$[CoNiC_3H_3N]^+ + [C_2H_6]$	10%	(23)
$\Sigma\, k = 2.5 \cdot 10^{-9}$ cm^3 s^{-1}			
$\phi = 0.80$			

modeling[1]) for the elimination of molecular H_2 was carried out with the following boundary conditions taken into account, which were defined by the experimental results. *i*) The different modes of dehydrogenation in the case of Fe_2^+ and $FeCo^+$ were considered by weight factors $f_{1,1}$ and $f_{1,2}$ for the 1,1- and 1,2-eliminations, respectively. *ii*) Because alkyl H-atoms do not equilibrate completely, the weight factor f_{scr} accounts for the extent of the H/D scrambling in the backbone; however, f_{scr} does not represent an additional, free parameter for the modeling but is determined by the parameters $f_{1,1}$ and/or $f_{1,2}$ ($f_{scr} = 1 - f_{1,1} - f_{1,2}$). *iii*) The equilibration of the H/D atoms does not necessarily include the complete alkyl chain for every cluster ion examined, but only part of it; this situation is taken into account by the statistical probabilities $p_{scr}(XY)$ (X, Y = H, D) to eliminate H_2/HD/D_2 only from those positions which are involved in the equilibration (*Table 4*). *iv*) Dehydrogenation is associated with a non-negligible kinetic isotope effect (KIE). With these conditions, the general algebraic structures of the

[1]) For a description of the technical details of the modeling procedure used, see [21a] and references cited therein.

Table 3. *Isotopic Patterns for the Dehydrogenation of Pentanenitrile by Fe_2^+, Co_2^+, Ni_2^+, $FeCo^+$, $FeNi^+$, and $CoNi^+$*[a])

	$-H_2$	$-HD$	$-D_2$	$-H_2$	$-HD$	$-D_2$	$-H_2$	$-HD$	$-D_2$
	Exp.			*Model 1*			*Model 3*		
11a/Fe_2^+	27	63	10	29.8	59.5	10.7	27.6	62.5	9.9
11b/Fe_2^+	59	41		55.2	44.3	0.5	58.7	40.9	0.4
11c/Fe_2^+	90	10		89.2	10.4	0.4	89.5	10.0	0.5
11d/Fe_2^+	90	10		89.2	10.4	0.4	89.5	10.0	0.5
				1.6/4.3[c])			0.5/1.7[c])		
	Exp.			*Model 2*			*Model 4*		
11a/Co_2^+	15	60	25	13.5	62.4	24.1	13.5	62.4	24.1
11b/Co_2^+	38	54	8	36.6	56.2	7.2	36.6	56.2	7.2
11c/Co_2^+	100			100			100		
11d/Co_2^+	100			100			100		
				1.6/2.4[c])			1.6/2.4[c])		
	Exp.			*Model 2*			*Model 4*		
11a/Ni_2^+	<10[b])	80	<10[b])	7.2	91.0	1.8	7.2	88.8	4.0
11b/Ni_2^+	<10[b])	80	<10[b])	10.1	89.3	0.6	10.3	88.3	1.4
11c/Ni_2^+	90	10		91.3	8.1	0.6	87.6	11.1	1.3
11d/Ni_2^+	90	10		91.3	8.1	0.6	87.6	11.1	1.3
				4.0/11[c])			3.7/8.9[c])		
	Exp.			*Model 1*			*Model 3*		
11a/$FeCo^+$	12	70	18	14.5	64.3	21.2	12.0	71.3	16.7
11b/$FeCo^+$	59	38	2	54.5	44.9	0.6	60.5	39.1	0.4
11c/$FeCo^+$	85	15		90.8	8.7	0.5	84.8	13.4	1.8
11d/$FeCo^+$	100			100			100		
				4.1/6.8[c])			1.2/1.8[c])		
	Exp.			*Model 2*			*Model 4*		
11a/$FeNi^+$	3	87	10	7.1	85.5	7.4	7.2	83.8	9.0
11b/$FeNi^+$	20	73	7[b])	19.6	78.2	2.3	19.9	77.4	2.7
11c/$FeNi^+$	100			100			100		
11d/$FeNi^+$	100			100			100		
				3.1/5.2[c])			2.8/4.4[c])		
	Exp.			*Model 2*			*Model 4*		
11a/$CoNi^+$	5[b])	90	5[b])	5.9	90.1	4.0	5.9	89.7	4.4
11b/$CoNi^+$	16	82	2	16.1	82.7	1.2	16.2	81.5	1.3
11c/$CoNi^+$	100			100			100		
11d/$CoNi^+$	100			100			100		
				0.6/1.0[c])			0.5/0.9[c])		

[a]) Intensities of the products are normalized to 100%. [b]) Lower limits derived from analysis of the noise level. [c]) Mean deviation/maximum deviation.

kinetic modeling with the ratios H_2, HD, and D_2 for Fe_2^+ and $FeCo^+$ (*Model 1*) and for Ni_2^+, Co_2^+, $FeNi^+$, and $CoNi^+$ (*Model 2*) are given by *Eqns. 24–29*, respectively.

Model 1:

$$H_2 = f_{1,1} \times p(H_2[\delta]) + f_{1,2} \times p(H_2[\delta\gamma]) + f_{scr} \times p_{scr}(H_2) \tag{24}$$

$$HD = \frac{f_{1,1} \times p(HD[\delta]) + f_{1,2} \times p(HD[\delta\gamma]) + f_{scr} \times p_{scr}(HD)}{KIE} \tag{25}$$

$$D_2 = \frac{f_{1,1} \times p(D_2[\delta]) + f_{1,2} \times p(D_2[\delta\gamma]) + f_{scr} \times p_{scr}(D_2)}{KIE^2} \quad (26)$$

Model 2:

$$H_2 = f_{1,2} \times p(H_2[\delta\gamma]) + f_{scr} \times p_{scr}(H_2) \quad (27)$$

$$HD = \frac{f_{1,2} \times p(HD[\delta\gamma]) + f_{scr} \times p_{scr}(HD)}{KIE} \quad (28)$$

$$D_2 = \frac{f_{1,2} \times p(D_2[\delta\gamma]) + f_{scr} \times p_{scr}(D_2)}{KIE^2} \quad (29)$$

While *Models 1* and *2* reproduce the experimental data reasonably well (*Table 3*), some significant discrepancies remain. For equilibrium isotope effects, it is known that they are usually close to unity and much smaller than KIEs of kinetically controlled reactions, because incorporation of a heavy isotope slows down the reaction both, in the forward as well as in the reverse direction such that the overall effects on the equilibrium constant K_{eq} are relatively small [22]. As this does not hold true for the KIEs, the latter are split into the individual contributions $KIE_{1,1}$, $KIE_{1,2}$, and KIE_{scr} to account for the possibility that the KIE associated with the 1,1-, 1,2-elimination, and the losses of H_2/HD/D_2 after equilibration, respectively, differ. With this refined approach, *Eqns. 24–26* and *27–29* change into *Eqns. 30–32* (*Model 3*) and *33–35* (*Model 4*), respectively, and the results of these calculations are in much better agreement with the experimental data (*Table 3*). The best fits obtained and the respective parameter sets for each model are given in *Table 4*.

Table 4. *Modeling Parameter Derived That Result in the Best Agreement with the Experimental Data*

	Positions of the alkyl chain involved in equilibration	*Models 1* and *2*				*Models 3* and *4*					
		KIE	$f_{1,1}$	$f_{1,2}$	f_{scr}	$KIE_{1,1}$	$KIE_{1,2}$	KIE_{scr}	$f_{1,1}$	$f_{1,2}$	f_{scr}
Fe_2^+	$\alpha, \beta, \gamma, \delta$	1.8 ± 0.2	0.16 ± 0.1	0.41 ± 0.1	0.43 ± 0.1	2.5 ± 1.1	1.9 ± 0.2	1.5 ± 0.1	0.24 ± 0.1	0.41 ± 0.1	0.35 ± 0.1
Co_2^+	γ, δ	1.3 ± 0.1		0.00 ± 0.1	1.00 ± 0.1		[a])	1.3 ± 0.1		0.00 ± 0.1	1.00 ± 0.1
Ni_2^+	$\alpha, \beta, \gamma, \delta$	1.4 ± 0.5		0.53 ± 0.2	0.47 ± 0.2		1.1 ± 0.4	0.6 ± 0.4		0.57 ± 0.2	0.43 ± 0.2
$FeCo^+$	β, γ, δ	1.7 ± 0.5	0.30 ± 0.1	0.40 ± 0.1	0.30 ± 0.1	3.7 ± 1.1	1.7 ± 0.2	0.8 ± 0.1	0.43 ± 0.1	0.35 ± 0.1	0.22 ± 0.1
$FeNi^+$	γ, δ	1.4 ± 0.5		0.53 ± 0.2	0.47 ± 0.2		1.7 ± 0.4	1.6 ± 0.4		0.57 ± 0.2	0.43 ± 0.2
$CoNi^+$	γ, δ	2.1 ± 0.1		0.72 ± 0.1	0.28 ± 0.1		2.1 ± 0.1	2.0 ± 0.1		0.72 ± 0.1	0.28 ± 0.1

[a]) Selective dehydrogenation without preceding scrambling most likely does not take place; therefore, the determination of $KIE_{1,2}$ is arbitrary.

Model 3:

$$D_2 = f_{1,1} \times p(H_2[\delta]) + f_{1,2} \times p(H_2[\delta\gamma]) + f_{scr} \times p_{scr}(H_2) \quad (30)$$

$$HD = \frac{f_{1,1} \times p(HD[\delta])}{KIE_{1,1}} + \frac{f_{1,2} \times p(HD[\delta\gamma])}{KIE_{1,2}} + \frac{f_{scr} \times p_{scr}(HD)}{KIE_{scr}} \quad (31)$$

$$D_2 = \frac{f_{1,1} \times p(D_2[\delta])}{KIE_{1,1}^2} + \frac{f_{1,2} \times p(D_2[\delta\gamma])}{KIE_{1,2}^2} + \frac{f_{scr} \times p_{scr}(D_2)}{KIE_{scr}^2} \quad (32)$$

Model 4:

$$H_2 = f_{1,2} \times p(H_2[\delta\gamma]) + f_{scr} \times p_{scr}(H_2) \quad (33)$$

$$HD = \frac{f_{1,2} \times p(HD[\delta\gamma])}{KIE_{1,2}} + \frac{f_{scr} \times p_{scr}(HD)}{KIE_{scr}} \quad (34)$$

$$D_2 = \frac{f_{1,2} \times p(D_2[\delta\gamma])}{KIE_{1,2}^2} + \frac{f_{scr} \times p_{scr}(D_2)}{KIE_{scr}^2} \quad (35)$$

The KIEs thus obtained are of the same magnitude as those reported in earlier C–H bond activation studies on various Fe^+ complexes [5d][21]. Furthermore, $KIE_{1,1}$ and $KIE_{1,2}$ associated with the selective 1,1- and 1,2-eliminations are on average slightly larger compared to the KIE_{scr} implied in the dehydrogenation after scrambling processes – especially for the 1,1-elimination – but not as significant as the difference between selective and scrambling processes found in other studies [21a]. In the case of Co_2^+, the calculated probabilities for H_2, HD, and D_2 eliminations, assuming a statistical H/D distribution at the γ and δ positions of **11a** and **11b**, and an associated KIE of 1.3 agree well with the experimental results. For Ni_2^+, the isotopic patterns for the products of dehydrogenation of **11a** and **11b** correspond to a classical *remote funtionaliziation* involving the γ and δ positions of the substrate; however, equilibration of every H(D) atoms in the backbone preceding dehydrogenation takes place with a contribution of almost 50%. The mode of dehydrogenation of pentanenitrile by $FeNi^+$ and $CoNi^+$ follows that of Co_2^+ and can be traced back to exclusive *remote functionalization* preceded by partial H/D exchange involving only the γ and δ positions with a higher ratio of selective 1,2-elimination in the case of $CoNi^+$ (*Table 4*).

Dehydrogenation of Pentanenitrile by Fe_2^+ and $FeCo^+$. In accord with the good agreement between the kinetic modeling and the experimental results, a possible explanation for the quite unexpected isotopic product patterns in the dehydrogenation of pentanenitrile by Fe_2^+ and $FeCo^+$ is provided by the operation of a formal 1,1-elimination of H_2 from the terminal C–H bonds in competition with the traditional 1,2-elimination mode. Although the former mode of bond activation is observed only rarely for late transition-metal ions, a few examples are known, *e.g.*, the C–H and the C–C bond activation of alkines by Mn^+ [23] and the dehydrogenation of a Me group of 1,3-dimethoxypropane by Fe^+ [24], with the latter example constituting a rare gas-phase variant of the *retro-Fischer–Tropsch* synthesis.

For Fe_2^+, the proposed mechanism for a 1,1-elimination of H_2 from the Me group of $CH_3(CH_2)_3CN$ is depicted in *Scheme 3*. After oxidative insertion of the Fe–Fe unit in the C–H bond at the δ position to generate the cyclic intermediate **17**, exocyclic C–H bond activation *via* the multi-center transition structure **18** is suggested to lead to molecular H_2 concomitant with formation of complex **19** as ionic product. With the shorter butanenitrile, an intermediate corresponding to **18** by initial insertion in a γ-

C–H bond no longer seems accessible. Instead, with butanenitrile, only the formation of the formal association complex $[Fe_2C_4H_7N]^+$, without indication for any bond activation reactivity, is observed. This behavior is consistent with the scenario proposed in *Scheme 3* in that the alkyl chain of butanenitrile is too short to assist the formation of cyclic species.

Scheme 3. *Model for the 1,1-Elimination from Pentanenitrile by* Fe_2^+

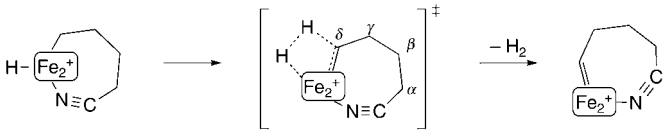

17 **18** **19**

Given that an exocyclic MCTS is energetically more favorable than an endocyclic variant, the 1,2-elimination of H_2 from pentanenitrile is suggested to proceed *via* an initial activation of a C–H bond in the γ position (*Fig. 2*; **20a**). The alternative δ-C–H bond activiation would lead to **17** (*Scheme 3*), from which an endocyclic MCTS had to be formed to bring about loss of H_2 *via* the 1,2-elimination mode. Although not rigorously proven, the initial activation at the γ position appears more plausible. However, while for the reaction of Fe_2^+ with pentanenitrile the intermediate **20a** (R = CH_3) is capable to undergo an additional exocyclic C–H bond activation step, from **20b** (R = H) elimination of H_2 would imply the formation of an endocyclic MCTS. This latter option does not seem to exist, and H_2 is generated neither from *n*-C_3H_7CN/Fe_2^+ nor from *n*-$C_3H_7CN/FeCo^+$ under thermal conditions.

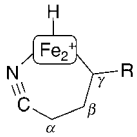

20a R = Me
20b R = H

Fig. 2. *Proposed structure for the intermediate resulting from the insertion of* Fe_2^+ *in the* γ*-C–H bond of pentanenitrile* (**20a**) *and butanenitrile* (**20b**)

As to the structural and electronic details of all of the RCN/MM'^+ species and their initial C–H bond activation intermediates discussed in this study, for the time being no reliable data are available, and appropriate computational investigations are indicated. This holds true in particular for the complexes with heteronuclear clusters, *e.g.*, $FeCo^+$, as for these systems quite a few interesting reaction scenarios with regard to the nature of the complexation as well as mechanistic details of activation steps are conceivable.

Reactions of Ni_2^+ *and* $CoNi^+$ *Including Some Specific Aspects of C–C Bond Activation.* In terms of product formation, Ni_2^+ shows the richest pattern of all clusters studied, and this is also enlarged in comparison to atomic Ni^+. For Ni_2^+, double dehydrogenation of pentanenitrile is observed with high efficiency, whereas simple dehydrogenation prevails for Ni^+ [5b,c]. This result is in accord with the multiple

dehydrogenation of butane by Ni_2^+ (up to three times), meanwhile atomic Ni^+ dehydrogenates this substrate only once [18].

In addition to dehydrogenation of pentanenitrile by Ni_2^+, ionic products with mass differences of $\Delta m = 29$ and 30 are observed, which correspond to the combined losses of $H_2 + HCN$ and $H_2 + C_2H_4$, respectively. Except for the combined H_2/HCN elimination, all other reaction channels of Ni_2^+ are also observed for $CoNi^+$. While the reaction efficiency of *n*-$C_4H_9CN/CoNi^+$ is the highest among all systems studied, the major part of reactivity is due to single dehydrogenation in the products formed by the $CoNi^+$ cluster, whereas for Ni_2^+ mainly double dehydrogenation is observed (*Table 2*).

The consecutive losses of HCN or C_2H_4 after dehydrogenation are proposed to occur as a result of the processes exemplified for Ni_2^+ in *Scheme 4:* after dehydrogenation and subsequent insertion in the C–CN bond (**21** → **22**) either a β-H (**22** → **23**) or a β-alkyl shift (**22** → **24**) take place, both involving an allylic position; because the product isotope distributions for **11c**/Ni_2^+ and **11d**/Ni_2^+ are the same, the β-H migration (**22** → **23**) quite probably is reversible.

Scheme 4. *Proposed Mechanism for the Eliminations of C_2H_4 and HCN, Respectively, from Pentanenitrile/Ni_2^+ Subsequent to Dehydrogenation*

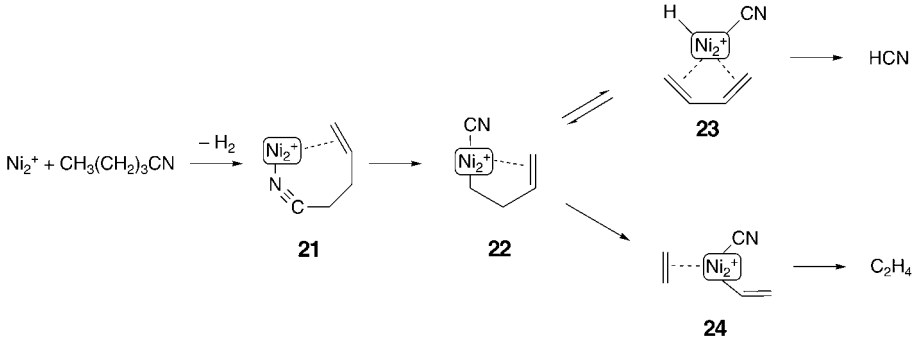

The resulting intermediates **23** and **24** then lead to the reductive elimination of HCN and the evaporation of C_2H_4, respectively. In agreement with these suggestions, the product ion $[Ni_2C_3H_3N]^+$, for example, undergoes the secondary *Reaction 36* in the presence of pentanenitrile. Quite possibly, the resulting ionic product $[Ni_2C_7H_{11}N]^+$ corresponds to a complex that contains an ethene and a pentenenitrile ligand, which are formed in course of HCN loss and bound to the Ni_2^+ core. Future studies are indicated to shed further light on questions like structural details or reactivity patterns of these novel metal cluster cations.

$$[Ni_2C_3H_3N]^+ + n\text{-}C_4H_9CN \rightarrow [Ni_2C_7H_{11}N]^+ + HCN \quad (36)$$

Insertion of a transition-metal cation in a C–CN bond has previously been discussed in a different context [25]. In these studies, the detailed electronic structure influence of the transition-metal cations Fe^+ through Cu^+ on their reactivities with 2-methylbutanenitrile were probed and three major processes were identified: *i*) *remote functionalization*, *ii*) initial insertion into the C–CN bond ('allylic mechanism') in

analogy to the mechanism depicted in *Scheme 4*, and *iii*) an ion/dipole mechanism, in which the N-atom remains coordinated to the transition metal throughout the entire reaction sequence. The latter mechanism, prevailing for the late transition-metal cations Cu^+ and Ni^+, might also be operative in the neutral products formed in *Reactions 13*, *14*, and *23* as an alternative to the allylic mechanism, depicted in *Scheme 4*.

For double dehydrogenation, the mechanism shown in *Scheme 5* is compatible with the experimental data. Starting from the complex **21**, reversible insertion in the allylic C–H bond leads to **25**, from which the second dehydrogenation may occur (**25** → **27**). Alternatively, reversible insertion in a C–H bond at the α position gives rise to the complex **26**; from the latter, after additional allylic C–H bond activation H_2 may be liberated to produce **27**. We note in passing that in the course of these reactions the *end-on* coordination mode indicated in structures **25**, **26**, and **27** most likely will change to a *side-on* coordination to the CN group.

Scheme 5. *Proposed Mechanism for the Double Dehydrogenation of Pentanenitrile by* Ni_2^+

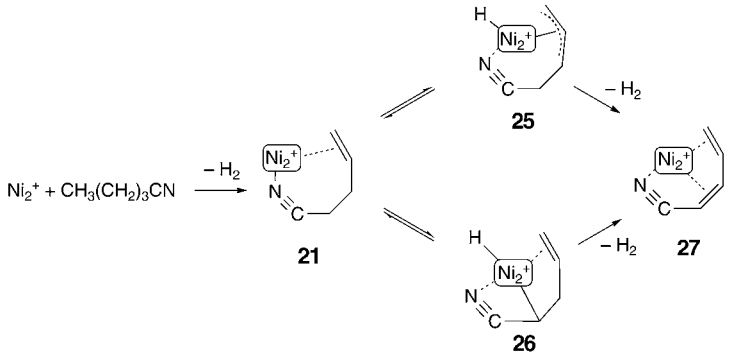

Secondary Reactions of Co_2^+, *FeCo*$^+$, *and FeNi*$^+$. Some secondary reactions observed in this study are noteworthy, and all are probably related to each other as well as to some of the primary reactions already mentioned above for Ni_2^+ and $CoNi^+$.

$$[Co_2C_5H_7N]^+ + n\text{-}C_4H_9CN \rightarrow [Co_2C_8H_{12}N_2]^+ + C_2H_4 \quad (37)$$

$$[FeCoC_5H_7N]^+ + n\text{-}C_4H_9CN \rightarrow [FeCoC_6H_{10}N_2]^+ + C_4H_6 \quad (38)$$

$$[FeNiC_5H_7N]^+ + n\text{-}C_4H_9CN \rightarrow [FeNiC_6H_{10}N_2]^+ + C_4H_6 \quad (39)$$

$$[FeNiC_5H_7N]^+ + n\text{-}C_4H_9CN \rightarrow [FeNiC_9H_{13}N]^+ + [CH_3N] \quad (40)$$

The product ion $[Co_2C_5H_7N]^+$ reacts with a second molecule of pentanenitrile to form the complex ion $[Co_2C_8H_{12}N_2]^+$ concomitant with loss of ethene (*Eqn. 37*). The possibility that the latter product ion is produced in a secondary reaction of the initially formed encounter complex $[Co_2C_5H_9N]^+$ with pentanenitrile, associated with the loss of intact ethane, can be excluded by a double-resonance experiment, in which after

continuous ejection of $[Co_2C_5H_7N]^+$ from the ICR cell a signal due to $[Co_2C_8H_{12}N_2]^+$ is no longer observed.

For $FeCo^+$, the secondary *Reaction 38* is observed, which is absent for the reactions of the homonuclear cluster ion Fe_2^+. Again, a double-resonance experiment proves that the product ion $[FeCoC_6H_{10}N_2]^+$ originates from the reaction of $[FeCoC_5H_7N]^+$ with pentanenitrile and is not due to a reaction of the initially formed encounter complex. $FeCo^+$ and $FeNi^+$ have in common that their primary dehydrogenation products react further with pentanenitrile (*Eqns. 38* and *39*). The secondary *Reaction 40* of $[FeNiC_5H_7N]^+$ with pentanenitrile exhibits a formal relationship of this cluster ion with *Reaction 13* of Ni_2^+ (*Table 2*). Obviously, the complexed cluster $[FeNiC_5H_7N]^+$ is capable to bring about in a secondary, multi-step process formation of both H_2 and HCN. Actually, also the reactions reported in *Eqns. 37–39* bear some resemblance to the primary reactions of Ni_2^+ with *n*-C_4H_9CN (*Eqns. 13* and *14*, *Table 2*, and *Scheme 4*).

Reactions of MM'^+ with Shorter Nitriles. The bond activation process of the shorter nitriles CH_3CN, C_2H_5CN, and *n*-C_3H_7CN are only observed for the Ni-containing clusters Ni_2^+, $FeNi^+$, and $CoNi^+$ (*Table 5*). The Ni-free clusters Fe_2^+, Co_2^+, and $FeCo^+$ activate neither any C–C nor C–H bonds; only the formation of the adduct complex $[MM'C_4H_7N]^+$ is observed in the reaction with the shorter butanenitrile. The higher reactivity of Ni_2^+ reported above for its reactions with pentanenitrile is also reflected in the behavior with the shorter butanenitrile as almost the same reaction channels are observed with both substrates, except that the combined elimination of H_2 and C_2H_4 from pentanenitrile is replaced by the simple evaporation of C_2H_4 from butanenitrile.

The additional *Reaction 41* of Ni_2^+ with pentanenitrile, in which surprisingly atomic Ni^+ is produced, is also observed for the shorter propanenitrile (*Eqn. 48*) as well as for ethanenitrile (*Eqn. 52*). With regard to thermochemical aspects, a straightforward explanation of these reactions is not at hand. While it is conceivable that the neutral product correspond to an inserted R–Ni–CN species which could help in improving the thermochemical deficit, up to now such a species has been neither observed nor considered in previous gas-phase or matrix-isolation studies [26]. Further, one has to consider that possibly long-lived excited states of Ni_2^+ are present, the existance of which may account for the results as well (see *Experimental*).

The crucial role of Ni in the chemistry of $FeNi^+$ and $CoNi^+$ is indicated by the similarity of the reactions of these clusters with the nitriles reported in *Table 5*. For example, dehydrogenation of *n*-C_3H_7CN is only observed for Ni_2^+, $FeNi^+$, and $CoNi^+$, and is completely absent in the reactions of Fe_2^+, Co_2^+, and $FeCo^+$. For $CoNi^+$, in comparison to $FeNi^+$, the similarity with Ni_2^+ is even more pronounced. In contrast to $FeNi^+$, C–C bond activation resulting in C_2H_4 evaporation occurs for the $CoNi^+$ and the Ni_2^+ clusters in their reactions with both *n*-C_3H_7CN and C_2H_5CN (*Eqns. 45*, *51*, *60*, and *63*).

Cluster Decomposition. Beside the similarities of the Ni-containing clusters Ni_2^+, $FeNi^+$, and $CoNi^+$ with regard to their reactions with nitriles shorter than pentanenitrile, it is worth mentioning that cluster-ion decomposition in primary reactions with the alkanenitriles examined here are exclusively observed for these three metal-cluster cations; for the remaining clusters Fe_2^+, Co_2^+, and $FeCo^+$ metal–metal bond cleavage only occurs in secondary reactions. These findings point to smaller bond energies between the two metal atoms in the Ni-containing clusters compared to Fe_2^+, Co_2^+, and

Table 5. *Reactions of the Homo- and Heteronuclear Cluster Cations MM'^+ (M, M′ = Fe, Co, Ni) with Butane-, Propane-, and Ethanenitrile, Respectively*

$Ni_2^+ + n\text{-}C_3H_7CN$	$Ni^+ + [NiC_4H_7N]$	2%	(41)
	$[Ni_2C_4H_5N]^+ + H_2$	57%	(42)
	$[Ni_2C_4H_3N]^+ + 2\,H_2$	28%	(43)
	$[NiC_4H_7N]^+ + Ni$	4%	(44)
	$[Ni_2C_2H_3N]^+ + C_2H_4$	8%	(45)
	$[Ni_2C_3H_4]^+ + H_2 + HCN$	1%	(46)
$\Sigma\, k = 2.07 \cdot 10^{-9}$ cm^3 s^{-1}			
$\phi = 0.62$			
$Ni_2^+ + C_2H_5CN$	$[Ni_2C_3H_5N]^+$	7%	(47)
	$Ni^+ + [NiC_3H_5N]$	13%	(48)
	$[Ni_2C_3H_3N]^+ + H_2$	20%	(49)
	$[NiC_3H_5N]^+ + Ni$	35%	(50)
	$[Ni_2CHN]^+ + C_2H_4$	25%	(51)
$\Sigma\, k = 1.38 \cdot 10^{-9}$ cm^3 s^{-1}			
$\phi = 0.39$			
$Ni_2^+ + CH_3CN$	$Ni^+ + [NiC_2H_3N]$	12%	(52)
	$[NiC_2H_3N]^+ + Ni$	77%	(53)
	$[Ni_2CN]^+ + CH_3$	11%	(54)
$\Sigma\, k = 1.27 \cdot 10^{-9}$ cm^3 s^{-1}			
$\phi = 0.32$			
$FeNi^+ + n\text{-}C_3H_7CN$	$[FeNiC_4H_7N]^+$	25%	(55)
	$[FeNiC_4H_5N]^+ + H_2$	40%	(56)
	$[NiC_4H_7N]^+ + Fe$	35%	(57)
$\Sigma\, k = 9.34 \cdot 10^{-10}$ cm^3 s^{-1}			
$\phi = 0.25$			
$CoNi^+ + n\text{-}C_3H_7CN$	$[CoNiC_4H_5N]^+ + H_2$	53%	(58)
	$[NiC_4H_7N]^+ + Co$	43%	(59)
	$[CoNiC_2H_3N]^+ + C_2H_4$	4%	(60)
$\Sigma\, k = 1.83 \cdot 10^{-9}$ cm^3 s^{-1}			
$\phi = 0.48$			
$CoNi^+ + C_2H_5CN$	$[CoNiC_3H_5N]^+$	$< 4\%$	(61)
	$[NiC_3H_5N]^+ + Co$	80%	(62)
	$[CoNiCHN]^+ + C_2H_4$	16%	(63)
$\Sigma\, k = 1.55 \cdot 10^{-9}$ cm^3 s^{-1}			
$\phi = 0.38$			
$CoNi^+ + CH_3CN$	$[NiC_2H_3N]^+ + Co$	100%	(64)
$k = 1.74 \cdot 10^{-10}$ cm^3 s^{-1}			
$\phi = 0.38$			

$FeCo^+$. This conclusion is supported by the, though limited, thermochemical data available for the naked clusters Fe_2^+, Co_2^+, $FeCo^+$, and Ni_2^+: the dissociation energies of $D_0(Fe^+ - Fe) = 262 \pm 7$ kJ mol^{-1} [27], $D_0(Co^+ - Co) = 265 \pm 10$ kJ mol^{-1} [28], and $D_0(Co^+ - Fe) = 276 \pm 29$ kJ mol^{-1} [29][2]) well exceed that of $D_0(Ni^+ - Ni) = 201 \pm 7$ kJ mol^{-1} [30]; for $FeNi^+$ and $CoNi^+$, the corresponding energies are unknown. Further, in

[2]) $D_0(Fe^+ - Co)$ is nearly identical to $D_0(Co^+ - Fe)$ due to the small difference in the ionization energies of Fe and Co; see Footnote 21 of [29].

the disintegration of the NiM^+ (M = Fe, Co) clusters, the charged Ni^+-atom sticks to the nitrile, while atomic Fe and Co are eliminated in their neutral states (*Eqns. 19*, *22*, *57*, *59*, *62*, and *64*). We note in passing that an interdependence of the bond energy $D_0(M^+ - M')$ between two different metal atoms in cluster cations and their reactivity has been reported previously. For example, FeV^+ with a large dissociation energy of $D_0(V^+ - Fe) = 314 \pm 21$ kJ mol^{-1} [31][3]) reacts neither with alkanes nor with linear alkenes, but only with strained cyclic alkenes; $CoFe^+$, $CuFe^+$, and $FeSc^+$ with dissociation energies of $D_0(Co^+ - Fe) = 276 \pm 29$ kJ mol^{-1} [29], $D_0(Cu^+ - Fe) = 222 \pm 29$ kJ mol^{-1} [32][4]), and $D_0(Fe^+ - Sc) = 201 \pm 21$ kJ mol^{-1} [33] also show no reactivity toward alkanes and only activate C–H bonds of higher alkenes starting with butene; in contrast, $FeMg^+$ with a dissociation energy of only $D_0(Fe^+ - Mg) = 142 \pm 21$ kJ mol^{-1} dehydrogenates even alkanes, starting from pentane [34].

Conclusions. – The reactions of the homo- and heteronuclear clusters MM'^+ (M, M′ = Fe, Co, Ni) with some linear nitriles show, at least superficially, many similarities. However, the behavior of these dinuclear clusters is very distinct from that of the corresponding atomic cations Fe^+, Co^+, and Ni^+. Whereas Fe^+, Co^+, and Ni^+ activate both C–H and C–C bonds of nitriles, and, in addition, follow some intriguing metal-specific mechanisms, the diatomic cluster cations only insert in C–H bonds in the initial activation step. From the more reactive Ni-containing cluster cations $FeNi^+$, $CoNi^+$, and Ni_2^+ – in comparison to dinuclear Ni-free clusters – the two latter ones activate C–C bonds after initial C–H bond activation. Further, for both the dinuclear as well as the atomic cations, the regioselectivity of C–H bond activation mainly follows the concept of *remote functionalization*. Quite likely, this is a consequence of a linear *end-on* arrangement of the atomic or dinuclear cluster cations to the nitriles investigated. However, subtle mechanistic variations which are supported by detailed modeling of the isotope distributions seem to be operative, and electronic structure calculations [35] are suggested to uncover the origin of these effects.

We are grateful to the *Deutsche Forschungsgemeinschaft* (*DFG*) and the *Fonds der Chemischen Industrie* for financial support.

REFERENCES

[1] K. Koszinowski, D. Schröder, H. Schwarz, *J. Am. Chem. Soc.* **2003**, *125*, 3676; K. Koszinowski, D. Schröder, H. Schwarz, *Organometallics* **2004**, *23*, 1132; K. Koszinowski, D. Schröder, H. Schwarz, *Angew. Chem., Int. Ed.* **2004**, *43*, 121; H. Schwarz, *Leopoldina Jahrbuch* **2004**, *49*, 397.

[2] K. Eller, H. Schwarz, *Chem. Rev.* **1991**, *91*, 1121; D. Schröder, C. Heinemann, W. Koch, H. Schwarz, *Pure Appl. Chem.* **1997**, *69*, 273; V. E. Bondybey, M. K. Beyer, *J. Phys. Chem. A* **2001**, *105*, 951; D. K. Böhme, H. Schwarz, *Angew. Chem., Int. Ed.* **2005**, *44*, 2336 and refs. cit. therein.

[3] P. Braunstein, J. Rosé, in 'Metal Clusters in Chemistry', Ed. P. Braunstein, L. A. Oro, P. R. Raithby, Wiley-VCH, Weinheim, 1999, Vol. 2, p. 616; R. D. Adams, B. Captain, *J. Organomet. Chem.* **2004**, *689*, 4521.

[4] S. P. J. Albracht, *J. Biochim. Biophys. Acta* **1994**, *1188*, 167; M. Pavlov, P. E. M. Siegbahn, M. R. A. Blomberg, R. H. Crabtree, *J. Am. Chem. Soc.* **1998**, *120*, 548; S. I. Lippard, I. M. Berg, 'Principles of Bioinorganic Chemistry', University Science Books, Mill Valley, California, 1994.

---

[3]) $D_0(Fe^+ - V) = 444 \pm 21$ kJ mol^{-1} [31].

[4]) $D_0(Fe^+ - Cu) = 234 \pm 29$ kJ mol^{-1} [32].

[5] H. Schwarz, *Acc. Chem. Res.* **1989**, *22*, 282; K. Eller, W. Zummack, H. Schwarz, *Int. J. Mass Spectrom. Ion Processes* **1990**, *100*, 803; c) K. Eller, W. Zummack, H. Schwarz, L. Roth, B. S. Freiser, *J. Am Chem. Soc.* **1991**, *113*, 833; d) J. Loos, D. Schröder, H. Schwarz, 'The Encyclopedia of Mass Spectrometry', Ed. N. M. M. Nibbering, Elsevier, New York, 2005, Vol. 4, p. 659.
[6] R. Breslow, *Acc. Chem. Res.* **1980**, *13*, 170.
[7] a) M. C. Holthausen, Ph.D. Thesis, TU Berlin, 1996, D83; b) M. C. Holthausen, G. Hornung, D. Schröder, S. Sen, W. Koch, H. Schwarz, *Organometallics* **1997**, *16*, 3135; c) G. Hornung, Ph.D. Thesis, TU Berlin, 1998, D83.
[8] K. Eller, H. Schwarz, *Int. J. Mass Spectrom. Ion Processes* **1989**, *93*, 243.
[9] S. Maruyama, L. R. Anderson, R. E. Smalley, *Rev. Sci. Instrum.* **1990**, *61*, 3686.
[10] M. Engeser, T. Weiske, D. Schröder, H. Schwarz, *J. Phys. Chem. A* **2003**, *107*, 2855.
[11] R. A. Forbes, F. H. Laukien, J. Wronka, *Int. J. Mass Spectrom. Ion Processes* **1988**, *83*, 23.
[12] K. Koszinowski, M. Schlangen, D. Schröder, H. Schwarz, *Eur. J. Inorg. Chem.*, accepted.
[13] D. Schröder, H. Schwarz, D. E. Clemmer, Y.-M. Chen, P. B. Armentrout, V. I. Baranov, D. K. Böhme, *Int. J. Mass Spectrom. Ion Processes* **1997**, *161*, 175.
[14] F. Nakao, *Vacuum* **1975**, *25*, 431; J. E. Bartmess, R. M. Georgiadis, *Vacuum* **1983**, *33*, 149.
[15] T. Su, *J. Chem. Phys.* **1988**, *89*, 4102; T. Su, *J. Chem. Phys.* **1988**, *89*, 5355.
[16] *fitfirstorder*, R. Berger, TU Berlin.
[17] M. B. Comisarow, V. Grassi, G. Parisod, *Chem. Phys. Lett.* **1978**, *57*, 413.
[18] T. F. Magnera, D. E. David, J. Michl, *J. Am. Chem. Soc.*, **1987**, *109*, 936.
[19] R. L. Hettich, B. S. Freiser, *J. Am. Chem. Soc.* **1987**, *109*, 3537.
[20] M. Schlangen, M. Diefenbach, C. van Wüllen, H. Schwarz, unpublished results.
[21] a) C. Trage, D. Schröder, H. Schwarz, *Organometallics* **2003**, *22*, 693; b) J. Loos, D. Schröder, W. Zummack, H. Schwarz, *Int. J. Mass Spetrom. Ion Processes* **2002**, *217*, 169.
[22] D. Schröder, R. Wesendrup, R. H. Hertwig, T. K. Dargel, H. Grauel, W. Koch, B. R. Bender, H. Schwarz, *Organometallics* **2000**, *19*, 2608.
[23] C. Schulze, H. Schwarz, *Chimia* **1987**, *41*, 202.
[24] T. Prüsse, A. Fiedler, H. Schwarz, *J. Am. Chem. Soc.* **1991**, *113*, 8335.
[25] K. Eller, W. Zummack, H. Schwarz, *J. Am. Chem. Soc.* **1990**, *112*, 621.
[26] T. S. Kurtikyan, V. T. Aleksanyan, *Doklady Akademii Nauk SSSR* **1977**, *236*, 1371.
[27] S. K. Loh, L. Lian, D. A. Hales, P. B. Armentrout, *J. Phys. Chem.* **1988**, *92*, 4009.
[28] D. A. Hales, C. X. Su, L. Lian, P. B. Armentrout, *J. Chem. Phys.* **1994**, *100*, 1049.
[29] D. B. Jacobson, B. S. Freiser, *J. Am. Chem. Soc.* **1984**, *106*, 4623.
[30] L. Lian, C.-X. Su, P. B. Armentrout, *J. Chem. Phys.* **1992**, *96*, 7542.
[31] R. L. Hettich, B. S. Freiser, *J. Am. Chem. Soc.* **1985**, *107*, 6222.
[32] E. C. Tews, B. S. Freiser, *J. Am. Chem. Soc.* **1987**, *109*, 4433.
[33] L. M. Lech, J. R. Gord, B. S. Freiser, *J. Am. Chem. Soc.* **1989**, *111*, 8588.
[34] L. M. Roth, B. S. Freiser, C. W. Bauschlicher Jr., H. Partridge, S. R. Langhoff, *J. Am. Chem. Soc.* **1991**, *113*, 3274.
[35] G. L. Gutsev, M. D. Mochena, P. Jena, C. W. Bauschlicher Jr., H. Partridge III, *J. Chem. Phys.* **2004**, *121*, 6785.

Received February 23, 2005